Research Article

Multi-Objective Design of An Induction Motor Using A New Method For Finding The Optimal Solution By The Pareto Front Based On Harmony Search

Idris LAOUAR[1],* , *Ahcene BOUKADOUM*[1]

[1]Department of Electrical Engineering, Laboratoire d'électrotechnique de Skikda «LES», Université du 20 Août 1955, 21000 Skikda, Algeria.

idris.laouar@univ-skikda.dz,a.boukadoum@univ-skikda.dz

*Corresponding author: Idris LAOUAR; idris.laouar@univ-skikda.dz

Abstract. *This article introduces a novel method for choosing the optimal solution from the Pareto front generated by the multi-objective harmony search (MOHS) algorithm, specifically aimed at optimizing an induction motor. We formulate both single- and multi-objective optimization problems that minimize active mass while maximizing efficiency and rated torque. To effectively identify and manage the Pareto-optimal front, we utilize non-dominated elitist fast sorting and crowding distance. Comprehensive simulations using MATLAB software were conducted on a 18.5 kW, 4-pole, 50 Hz squirrel-cage induction motor serving as our test system. Furthermore, in-depth comparisons were made between our proposed method and established approaches like the fuzzy membership approach and the geometric mean, all vying to select the best solution from the Pareto set generated by the Harmony search algorithm. This rigorous evaluation highlighted the superior efficiency and robustness of our method, demonstrating significant improvements compared to the motor's initial values: 0.4377% for rated torque, 0.1766% for efficiency, and a remarkable 7.1048% for active mass.*

Keywords

induction motor design. active mass minimization. efficiency maximization. torque rating maximization. Harmony search algorithm. fuzzy membership approach. Geometric Median

1. Introduction

Induction motors are extensively used in electrical power industry. There is a growing interest for achieving optimal designs that enhance their performance and energy efficiency. Designers strive to improve crucial factors such as starting and rated torque, efficiency, and power factor, etc [1].

The geometric dimensions of the induction motor, including stator and rotor slots, as well as core length, play a vital role in overall performance. Stator slots design optimization, for example, can enhance efficiency and reduce harmonic losses [2]. The number of rotor slots influences induction torque performance, and increasing the axial length of the core can provide a simple solution for enhancing efficiency [3]. Therefore, optimizing motor geometry is essential for improving overall performance.

In recent years, nature-inspired metaheuristic optimization algorithms, such as the Harmony Search (HS) algorithm, that have gained popularity for optimizing induction motor designs [4]. The HS algorithm, initially proposed by Zong Woo Geem et al. in 2001 [5], has become a preferred choice among heuristic search algorithms for single-objective problems in various sci-

entific and technical domains [6]. A notable trend in research is the application of the HS algorithm to multi-objective problems, which poses a challenge for the future [7]. Previous applications of the HS algorithm to multi-objective problems, as presented in [8, 9], relied on the weighting method. However, Xu et al. developed the first multi-objective HS algorithm in [10], aiming to generate a set of Pareto-optimal front solutions. They successfully applied this algorithm to a robotic model and obtained a Pareto-optimal front consisting of five points.

In the context of induction motor design, the multi-objective nature of the problems introduces multiple objective functions that often conflict with each other. Improving one function may lead to the deterioration of another, making it impossible to find a single solution that optimizes all functions simultaneously. Consequently, it becomes necessary to identify a set of solutions that meet specific requirements, where each solution in the Pareto-optimal front is not dominated by other solutions [11].

However, even after obtaining the Pareto-optimal front, the challenge remains to select the most balanced solution among the objective functions relative to other solutions in the Pareto front. This selection process demands careful evaluation and a deep understanding of the trade-offs between conflicting objectives. The aim of this article is to find a solution that represents the best possible balance among the different objective functions in the Pareto front, considering the specific specifications and requirements of the induction motor. To accomplish this, a mathematical method has been proposed to identify a more balanced solution among the objective functions, and it has been compared with the Fuzzy Membership Approach applied in [12,13] and the Geometric Median method. This selection step is crucial to achieve an optimal solution based on problem priorities and constraints.

The structure of this work is as follows: Section 2. models the geometry of the induction motor and determines the objective functions. Section 3. provides an overview of the harmonic search optimization algorithm used to optimize the selected problem and explains the proposed method. Section 4. examines the results obtained using HS optimization and compares them with conventional designs. The final section is the conclusion.

2. Design of Induction Motor

This section summarizes the methods used to calculate the three objective functions (active mass, rated torque, and efficiency) for optimizing the squirrel cage induction motor. To model and optimize the selected functions, two steps need to be gone through: The first step to be done is the conventional design followed according to the procedure given in [14] and [15]. Then, a comparison is made to validate the results obtained by the conventional design with the required specifications of the induction motor as shown in Table 1.

Tab. 1: Specifications of the squirrel cage motor by the initial model and conventional design.

Model	T1A 180M-4	Conventional design
The rated output power (KW)	18.5	
The tension (V)	690	
The connections	Y	
Numbers of phases	3	
Frequency (Hz)	50	
The rated speed min-1	1460	1459.27
The rated torque (N.m)	121.01	121.07
Efficiency%	90.5	90.57
The power factor	0.86	0.861
The rated current (A)	19.89	19.84
The outer diameter (mm)	279	266.55

The main specifications are presented in Table 1. They include output power, voltage, connections, number of phases, and frequency, which are considered inputs for conventional design. In addition, the remaining parameters demonstrate that there is an approximation to the original model, so this shows that the algorithm used in the conventional design is valid for use as an optimization problem in the next section.

The second step modeled the main dimensions of the stator, the stator winding, the main dimensions of the rotor, and the end rings to make the optimal design.

2.1. Stator geometry

The stator geometry has important parameters for the design of perfect motors, based on the core outer and inner diameter and the slot geometry as shown in Figure 1.
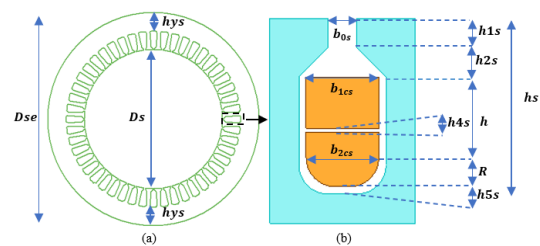
Fig. 1: Cross-section of the stator. (a) stator dimensions, (b) stator slot dimensions.

As a preliminary step, determine the equivalent core length represented as the motor's main dimension. in [15], the equivalent core length has a relationship with the main flux distribution, which remains approxi-

mately constant over a distance from the core and gradually decreases to zero along the machine shaft due to the effect of the edge field. Thus, the equivalent core length can be approximated by the following equation:

$$le = l + 2 * \delta, \tag{1}$$

Where (l) is the active core length, (δ) the air gap length. The air-gap diameter is the second main dimension of the motor and is determined by the following equation:

$$De = \chi * le, \tag{2}$$

Where (χ) the ratio between the equivalent length of the machine and the diameter of the air gap, it is estimated for the asynchronous machine by this relation $\chi = \frac{\pi}{2*p} \sqrt[3]{p}$, Where (p) the pair number of poles. Thus, the inner diameter of the stator obtained by this equation:

$$Ds = De + \delta. \tag{3}$$

In Figure 1 part (a) it is shown that the outer diameter of the stator has a relation with the following three parameters: inner diameter which is already shown in equation (3), the height of the yoke and the stator slot height. So, to determine the outer diameter it is necessary to calculate the slot height and the stator yoke height.

Part (b) of Figure 1 illustrates the type of slot that is chosen for this article, which is a semi-closed trapezoidal slot. The use of semi-closed slots results in low tooth loss and much quieter operation than with open slots.

The following equations present the main parameters of the slot, starting with the slot height of the stator:

$$h_s = h_{1s} + h_{2s} + h + R + h_{5s}, \tag{4}$$

where (h_{1s}) the height of the slot opening (h_{2s}) the height of the wedge, $(h$ and $R)$ the total height of the stator slot coil, (h_{5s}) the height of the slot inlay. In addition, the total width of the coil in the slot end of the stator expressed by the following expression:

$$b_{2cs} = b_{1cs} + \frac{2 * \pi * h}{Q_s}, \tag{5}$$

where (b_{1cs}) total coil width in stator slot opening, (Q_s) number of stator slots.

The values (S_{cus}), (S_{cs}), (S_s) are designated as the total area of the stator slot coil, the area of the conductor in the stator slot and the area of the stator slot,

respectively, and are given by,

$$\begin{cases} A_{scup} = \dfrac{(b_{1cs} + b_{2cs})}{2} * (h - h_{4s}), \\[2mm] A_{scd} = \dfrac{\pi * R^2}{2} + (b_{2cs} - 2 * R) * R, \\[2mm] S_{cus} = A_{scup} + A_{scd}, \\[2mm] S_{cs} = \dfrac{S_{cus} * k_{cus}}{Z_{Q_s}}, \end{cases} \tag{6}$$

and

$$\begin{cases} b_{1s} = b_{1cs} + 2 * h_{5s}, \\[1mm] b_{2s} = b_{2cs} + 2 * h_{5s}, \\[1mm] R_s = R + h_{5s}, \\[1mm] A_{sup} = b_{0s} * h_{1s} + \dfrac{(b_{0s} + b_{1s})}{2} h_{2s} + \dfrac{(b_{1s} + b_{1s})}{2} h, \\[1mm] A_{sd} = \dfrac{\pi * R_s^2}{2} + (b_{2s} - 2 * R_s) * R_s, \\[1mm] S_s = A_{sup} + A_{sd}, \end{cases} \tag{7}$$

where (b_{1s}) and (b_{2s}) are Width of lower and upper slots respectively, k_{cus} is the space factor inside the stator slot insulation and (Z_{Q_s}) is the number of conductors per slot. The height of the stator yoke expressed by the following equation:

$$hys = \frac{\hat{\varphi}_m}{2 * k_{fe} * l * \hat{B}_{ys}}, \tag{8}$$

where (k_{fe}) is space factor for iron, $(\hat{B}_{ys})$ is the maximum flux density at the stator yoke, $(\hat{\varphi}_m)$ is the maximum magnetic flux per phase and (N) is the number of conductors per phase, are denoted by the following expression respectively:

$$\hat{\varphi}_m = \frac{\sqrt{2} * E_m}{w * k_{ws} * N},$$
$$N = \frac{Q_s * Z_{Qs}}{2 * a * m}, \tag{9}$$

where (E_m) is the induced EMF of the stator phase for induction motors, which is $(0.93 - 0.98)Us$, (Us) is the fundamental terminal voltage, (w) is the angular velocity of the generated current or voltage, and (k_{ws}) is the winding factor for stator, (m) is the number of phases and (a) is the number of parallel branches.
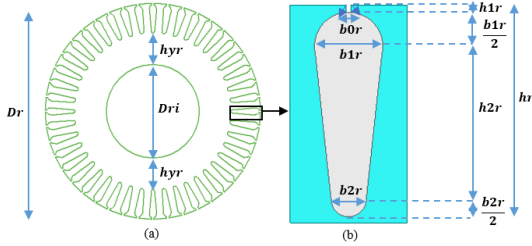
So, the outer diameter is defined by the following equation:

$$Dse = Ds + 2 * (hs + hys. \tag{10}$$

In [14], the best theoretical diameter ratio (the ratio of stator inner diameter to outer diameter, Ds/Dse) is about $(0.6 - 0.67)$, take this range is taken as a constraint for optimising the stator inner and outer diameter geometries.

2.2. Rotor geometry

In the same way, important parameters of the rotor part are presented, which are based on the size of the core and slot. Figure 2 illustrates the type of slot and the different rotor parameters.

Fig. 2: Cross-section of the rotor (a) rotor dimensions, (b) rotor slot dimensions.

The outer diameter of the rotor is expressed by the following expression:

$$Dr = De - \delta. \qquad (11)$$

The following equations present the main parameters of the rotor slot as shown in Figure 2-part b, starting with the rotor slot height:

$$h_r = h_{1r} + \frac{b_{1r}}{2} + h_{2r} + \frac{b_{2r}}{2}, \qquad (12)$$

where (h_{1r}) the opening height of the rotor bar, $(b_{1r}$ and $b_{2r})$ the opening width and the end of the rotor bar, (h_{2r}) the height between opening width and end of the rotor bar.

Where end width of the rotor bar expressed by the following expression:

$$b_{2r} = b_{1r} - \frac{2 * \pi * h_{2r}}{Q_r}, \qquad (13)$$

where (Q_r) is the rotor bar number.

The values (S_{alr}), (S_r) are designated as the conductor area in the rotor bar and the area of the rotor slot, respectively, and are given by,

$$\begin{cases} S_{alr} = \frac{(b_{1r} - b_{2r})}{2} * h_{2r} + \frac{\pi * b_{1r}^2}{8} + \frac{\pi * b_{2r}^2}{8}, \\ S_r = b_{0r} * b_{1r} * S_{alr}. \end{cases} \quad (14)$$

The height of the rotor head is expressed by the following equation:

$$hyr = \frac{\hat{\varphi}_m}{2 * k_{fe} * l * \hat{B}_{yr}}, \qquad (15)$$

where $(\hat{B}_{yr})$ is the maximum flux density at the rotor yoke.

In Figure 2 part (a) it shows that the inner diameter of the rotor has a relation with the following three parameters: rotor outer diameter, the height of the yoke and the height of the rotor slot. Therefore, it is defined by the following equation:

$$Dri = Dr - 2 * (hr + hyr). \qquad (16)$$

2.3. Objective functions

This part shows the relationship with the previous part that is expressed the objective functions on the efficiency of both the rated torque and the active mass to improve the IM. Moreover, it is difficult to achieve a precise evaluation of the performance of the motor in the real world, so constraints must be made to avoid electrical or magnetic transgressions. Therefore, his section presents a detailed description for objective functions mentioned to optimize IM.

1) Efficiency (η)

The efficiency of a motor is a percentage of energy transformed from a machine, so the increase in this percentage represents decrease on the energy losses of the motor and that's why there should be a subject put it as an objective in most optimization study. It is defined by the ratio of output power to input power, and is calculated from the total loss of the induction motor. So, it is defined by the following equation:

$$\eta = \frac{P_{out}}{P_{in}} = \frac{P_{out}}{P_{out} + P_{in}}, \qquad (17)$$

where

$$P_{tot} = P_{fe} + P_{cus} + P_{alr} + P_m + P_{add}, \qquad (18)$$

where (P_{in}) is electrical power, (P_{out}) is mechanical power, (P_{fe}) is iron losses, (P_{cus}) is stator winding losses, (P_{alr}) is rotor bar losses, (P_m) is mechanical losses, and (P_{add}) is additional losses.

• Iron losses

In [16], the losses in the iron are related to the frequency. In the case of low frequency, generally the losses structure is generated in the teeth and yoke of the stator and only few in the rotor. The latter can be neglected due to the low frequency of the rotor. In the second case at high frequencies, it should be noted that these losses cannot be neglected as shown in [17]. The losses in the stator iron are calculated by an analytical method as was used in [18, 19]. Thus, the stator yoke losses P_{fey}, and the stator teeth P_{fed}, are expressed by

the following equations:

$$\begin{cases} P_{fey} = k_{fe,y} * P15 * \left(\dfrac{f}{50Hz}\right)^{1.5} * \left(\dfrac{\hat{B}_y}{1.5T}\right)^2 * m_y, \\ P_{fed} = k_{fe,d} * P15 * \left(\dfrac{f}{50Hz}\right)^{1.5} * \displaystyle\sum_n \left(\dfrac{\hat{B}_{d,n}}{1.5T}\right)^2 * m_{d,n}, \end{cases}$$
$$\tag{19}$$

where $P15$ is the iron loss factor, $k_{(}fe,d)$, $k_{(}fe,y)$ correction coefficient of iron losses in the stator teeth and yoke, estimated by a value 1.8, 1.6 respectively, $\hat{B}_{d,n}$, $\hat{B}_y$ is the maximum flux density in the stator teeth and yoke, with $m_{d,n}$, m_y is the mass of the teeth and yoke respectively. Figure 3 shows that there are different widths in the teeth, since for each width a different magnetic density is required to calculate all alone and n are the different parts of the magnetic induction in the tooth. The laminated steel material used in this article for the squirrel cage induction motor is M800-50A.
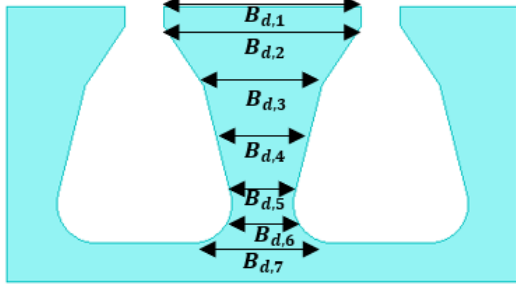

Fig. 3: Induction distribution in a tooth.

The sum of P_{fey}, and P_{fed}, gives the total iron losses P_{fe}. Now we try to acquire the iron loss resistance R_{fe}. We use the following equations:

$$P_{fe} = P_{fed} + P_{fey}, \tag{20}$$

$$R_{fe} = \frac{m * (E_m)^2}{P_{fe}}. \tag{21}$$

● **Losses in the stator winding and Losses in the rotor bar**

The Joule losses of the conductor windings in the stator slots and the Joule losses of the rotor bars are defined by the following equations:

$$\begin{cases} P_{cus} = m * R_s * I_s^2, \\ P_a lr = m * R_r' * I_r'^2, \end{cases} \tag{22}$$

$$\begin{cases} l_{av} = l + 1.2 * \left(\pi * \dfrac{Ds+hs}{2*p} * \dfrac{y}{y_Q}\right) + 0.05 \\ P_a lr = m * R_r' * I_r'^2, \\ Rs = \dfrac{N * 2 * l_{av}}{a * \sigma_{(}s80^o) * Scs}, \\ R_r' = \dfrac{\rho * \left(l + \frac{D_{ring}*m*S_{alr}}{\pi*p*Sr}\right)}{S_{alr} * \sigma_{r80^o}}, \end{cases} \tag{23}$$

where (y_Q, y) are stator pole pitch in slot pitches and Coil width in slot pitches respectively, (I_s^2, I_r') are stator and rotor currents, (l_{av}) is the average length, (D_{ring}) is Average diameter of the short-circuit ring, (ρ) is the factor for referring the rotor compounds to that of the stator in a squirrel cage induction motor, this is written as

$$\rho = \frac{4 * m}{Qr} * \left(\frac{Kws * N}{Kwr}\right)^2. \tag{24}$$

Equation (23) was used to obtain the copper resistance of the stator and the aluminum resistance of the rotor of the induction motor. Where (Kwr) is the winding factor for rotor, $(\sigma_{s80^o}, \sigma_{r80^o})$ is the value of conductivity at an ambient temperature of 80^oC we take this value for the hot resistance. Since the resistance increased with the increase of the temperature of the stator winding or the rotor bars. we posed that the temperature is a constant value 80^oC, because the variation of this component requires convoluted calculations that cannot be included in the electromagnetic model.

To determine the current in the stator phase, the equivalent circuit of an induction motor can be used as [20]. I_s is calculated by a simple division of the input voltage in the phase by the total equivalent impedance;

$$I_s = \frac{Vs}{Z_{eq}}, \tag{25}$$

where;

$$\begin{cases} y_m = \dfrac{1}{R_{fe}} - j\dfrac{1}{wL_m}, \\ Z_m = \dfrac{1}{y_m}, \\ Z_s = Rs + jwL_{\sigma s}, \\ Z_r' = \dfrac{R_r'}{s} + jwp\left(L_{bar} + \dfrac{L_{ring}}{2 * \sin^2\left(\frac{\pi p}{Qr}\right)}\right), \\ Z_{eq} = Z_s + \dfrac{Z_r' * Z_m}{Z_r' + Z_m}, \end{cases} \tag{26}$$

Where (s) is slip, $(L_{\sigma s}, L_m)$ is the stator leakage inductance and the magnetic inductance respectively, both of which are well detailed in [15,16], (L_{bar}, L_{ring}) is the bar leakage inductance and the end ring respectively, defined and expressed in [19].

Thus, the value of the current in the rotor of the equivalent circuit transferred to the stator side is;

$$I_r' = \frac{Em}{Z'r}. \tag{27}$$

● **Mechanical and additional losses**

The mechanical losses P_m, are due to the friction of the rotor bearings and the forced ventilation of the motor

structure. in [15], the mechanical losses are based on the synchronous speed ns, the outer rotor diameter D_r and the degree of protection of the motor (IP 55). It is defined as follows:

$$P_m = k_\rho * D_r * (l * +0.6 * \tau_p) * (\pi * D_r * ns)^2, \quad (28)$$

where k_ρ is an experimental factor for small and medium machines estimated at 15 and τ_p is the pole pitch.

Additional losses P_{add} represents all the remaining losses like harmonic losses, rotor iron losses, skin effect losses etc. Most of these losses are neglected but when they are collected, they have a considerable value e.g., in the squirrel cage motor the value of additional losses 0.3-2% per for the input power.

In [16], there is a connection between the additional losses and the input and output powers, it is defined by the following equation:

$$P_{add} = \left(0.025 - 0.005 * \log \left(\frac{Pout}{1kw} \right) \right) * Pin. \quad (29)$$

2) Rated torque T_u

The rated torque is the force generated by the rotation in a motor to drive the loads, so it is an important element to be put as a second objective function to improve. In addition, the rated torque is related to the resistive losses of the rotor and the mechanical loss that is generated by the reverse torque of the direction of rotation by friction. So, it can be expressed by the following equation:

$$T_u = \frac{\frac{P_{alr}}{s} - P_m}{2 * \pi * n_s}. \quad (30)$$

3) Mass active in the machine W_a

The third objective function is the active mass or mass of the materials used in the electrical and magnetic circuit. This component is not less important than the efficiency and the rated torque, because the increase of the mass of the active materials causes the efficiency and the cost of the motor to increase, the same thing if the mass decreases creating a decrease in the efficiency and the cost. So, the mass of the active materials is set as an objective function to take a minimum mass with optimum efficiency.

The mass of the active materials is divided into three parts: 1- the mass of the iron cores in the stator and rotor. 2- the mass of the conductor in the stator. 3- the mass of the bars and rings in the rotor. So, it can be expressed by the following equation:

$$W_a = W_{fe} + W_{cus} + W_{alr}. \quad (31)$$

At the beginning it starts with the iron mass that is built into the teeth and yokes of the stator and rotor, which is defined by the following equations:

$$\begin{cases} W_{fes} = \rho_{fe} \left(\dfrac{\pi * k_{fe} * l * (D_{se}^2 - D_s^2)}{4} \right. \\ \qquad\qquad \left. - k_{fe} * l * S_s * Q_s \right), \\ W_{fer} = \rho_{fe} \left(\dfrac{\pi * k_{fe} * l * (D_r^2 - D_{ri}^2)}{4} \right. \\ \qquad\qquad \left. - k_{fe} * l * S_r * Q_r \right). \end{cases} \quad (32)$$

The sum of W_{fes}, and W_{fer}, gives the total mass of iron W_{fe}, so this is defined as:

$$W_{fe} = W_{fes} + W_fer, \quad (33)$$

where ρ_{fe} is the density of the material of the iron.

The total mass of the conductor in the stator is related to the number of slots, the number of conductors in the slot, the density of material used as in this study used copper ρ_{cu} and total length for a single conductor. This mass is expressed by the following equation:

$$W_{cus} = \frac{\rho_{cu} * Q_s * Z_{Qs} * S_{cs} * 2 * l_{av}}{2}. \quad (34)$$

In the same way, it expresses the mass of the conductor in the rotor which is divided into two parts: the mass of the bars and the mass of the rings expressed by the following equation:

$$W_{alr} = W_{albar} + W_{alring}, \quad (35)$$

where

$$\begin{cases} W_{albar} = \rho_{al} * Q_r * S_{als} * l, \\ W_{alring} = \rho_{al} * 2 * \pi * D_{ring} * \left(S_r * \dfrac{Q_r}{2 * m * p} \right), \end{cases} \quad (36)$$

where ρ_{cu} , ρ_{al} are the material density of the copper and aluminum respectively.

After expressing the different objective functions selected, the following expression was used to maximize the three objective functions:

$$f = \max(\eta, T_{u'} - W_a). \quad (37)$$

2.4. The constraints and variables

To optimize the performance of a motor in the design, there are several constraints to be taken into account. In this work, the optimization constraints used for the induction motor are defined in Table 2.

The design parameters and their limit values have been given in Table 3 for the induction motor which is already presented in Table 1.

Tab. 2: Design constraints.

Magnetic Density in the air gap (T)	$0.7 < \hat{B}_\delta < 0.9$
The magnetic density in the stator teeth (T)	$1.4 < \hat{B}_{ds} < 2.1$
The magnetic density in the rotor teeth (T)	$1.5 < \hat{B}_{dr} < 2.2$
The current density in the stator conductors (A/mm^2)	$3 < \hat{J}_s < 8$
The current density in the rotor bars (A/mm^2)	$3 < \hat{J}_r < 6.5$
The power factor	$\cos\phi > 0.86$
The ratio between the inner and outer diameter of the stator	$0.6 < \frac{D_s}{D_{se}} < 0.67$
Starting torque (N.m)	$T_{st} > 99$

Tab. 3: Design parameters and limitations.

Design parameter	Lower limit	Upper limit
Z_{Qs}	20	48
$l(mm)$	145	180
$\delta(mm)$	0.2	2.5
$h(mm)$	16	26
$b_{1cs}(mm)$	4	8.5
$h_{2r}(mm)$	10	22
$b_{1r}(mm)$	4.5	9
$E_m(V)$	370.48	386.42
$\hat{B}_{ys}(T)$	1.4	2
$\hat{B}_{yr}(T)$	1	1.9

3. HS multi-objective algorithms and the proposed method

This set of solutions is called the Pareto front. In this section it has been explained how to find the optimum solution in the Pareto set by using the HS multi-objective algorithm.

3.1. AN OVERVIEW OF THE ALGORITHM Research harmony

The Harmony Search Algorithm (HS) is a heuristic search algorithm that is inspired by the process of music creation and the search for harmony in music. The harmony search algorithm uses a probabilistic approach to find optimal solutions for a given problem. It is based on the idea that when a musician plays a note, he tries to find harmony with the other notes played by the other musicians. In a similar way, the harmony search algorithm tries to find harmony between different possible solutions for a given problem, selecting those that are the most promising. It is also often used as an alternative to other heuristic search algorithms, such as the genetic algorithm and search Tabou algorithm, as it has many advantages in terms of simplicity and speed of convergence.

Multi-objective harmony search uses the same principle as simple harmony search, but based on several objectives rather than just one. This means that the algorithm looks for a solution that simultaneously optimizes several objectives, rather than just one. The detailed description of the optimization procedure of the HS multi-objective algorithm is given in [21], so in this section a brief explanation of Multi-Objective Harmony Search is given in the following steps:

1) Initialization of the parameters of the HS algorithm

The first step in starting the algorithm is to set the main parameters of the HS algorithm. These are the size of the harmony memory (HMS), the harmony consideration rate (HMCR), the pitch adjustment rate (PAR) and the number of improvisations (NI) it indicates the number of iterations.

2) Initialization of the harmony memory

The second step is the identification of a key element of the harmony search algorithm which is the harmony memory. Harmony memory (HM) is a key concept used in harmony search algorithms, such as the single-objective or multi-objective harmony search algorithm. In addition, the harmony memory plays an important role in the harmony search algorithm, as it stores the best solutions found so far and uses them as a reference for the search of new solutions. The HM can be represented as follows:

$$HM = \begin{bmatrix} x_1^1 & x_2^1 & \ldots & x_n^1 \\ x_1^2 & x_2^2 & \ldots & x_n^2 \\ \vdots & \vdots & & \vdots \\ x_1^{HMS} & x_2^{HMS} & \ldots & x_n^{HMS} \end{bmatrix}, \quad (38)$$

where $[x_1^i \quad x_2^i \quad x_n^i](i = 1, 2, \ldots, HMS)$ is the solution vector.

3) Improvisation of a new harmony from the HMm

The third step uses the three rules: (1) memory consideration (HMCR), (2) pitch adjustment (PAR) and (3) random selection, to generate a new harmony vector $x' = (x'_1, x'_2, \ldots, x'_n)$.

The harmony memory consideration rate (HMCR), determines the probability that an element of the harmony memory (x'a solution previously found from $(x^1 - x^{HMS})$) is used to generate a new solution in the next iteration of the algorithm. The more the rate of consideration of the harmony memory is generally varied between 0 and 1, is the rate of choosing a value from HM, while (1-HMCR) is the rate of randomly selecting a value from the range of possible values, as

shown in (39)

$$x'_i = \begin{cases} x'_i \in (x_i^1 \quad x_i^2 \dots x_i^{HMS}), rand \leqslant HMCR \\ x'_i \in x_i, \qquad\qquad\qquad else, \end{cases} \quad (39)$$

where rand is a uniform random number between [0 1] and $x_i = (Ub_i - Lb_i) * rand + Lb_i$, where $Lb \& Ub$ are the lower and upper bounds of the specific variable.

Pitch Adjustment (PAR) refers to the modification of the value of the solution vector (or "harmony") found by the Harmony Memory Consideration Rate (HMCR) in order to find new optimal solutions, the following expression is given:

$$x'_i = \begin{cases} x'_i \pm rand * bw, & rand \leqslant HMCR \\ x'_i, & else, \end{cases} \quad (40)$$

Where bw is the bandwidth. There are different formulas for bw in this paper we have used the formula proposed by Tuo et al [22].

4)   Classification of solutions in the harmony memory

The updating of the harmony memory in the HS algorithm from which the ranking is performed may differ between single-objective and multi-objective problems. In the case of a single-objective problem, the ranking of solutions can be performed using a single quality criterion value, and in the case of a multi-objective problem, the ranking of solutions can be performed using several quality criterion values simultaneously. However, there are a number of ranking strategies to drive the generation of higher quality Pareto fronts for multi-objective problems [23]. In this work, to find Pareto optimal solutions we used the ranking proposed by Deb et al [24].

5)   Stopping criterion

The HS algorithm is stopped when the number of improvisations (NI) has been reached. Otherwise, sections 3.1.3 and 3.1.4 are repeated.

6)   Best compromise solution

Obtaining the Pareto optimal set is a crucial first step, but choosing the best solution among them is a complex issue. Fortunately, many methods have been developed to identify the best compromise solutions, also known as preferred solutions. Reference [25] provides an overview of these methods.

In this paper, the fuzzy set method, the geometric median, and the proposed method are used to determine the best compromise solution from the obtained Pareto front.

a)   Fuzzy membership approach

A fuzzy decision-making approach, inspired by references [12-13], is employed to identify the best compromise solution. The method consists of two main steps: (1) implementing fuzzy-based mechanisms and (2) calculating normalized membership values.

- Perform fuzzy-based mechanisms:

$$\mu_o = \begin{cases} 0, & f_0 \leqslant f_0^{\min} \\ \dfrac{f_0 - f_0^{\min}}{f_0^{\max} - f_0^{\min}}, & \leqslant f_0^{\min} < f_0 < f_0^{\max} \\ 1, & f_0 \geqslant f_0^{\max} \end{cases} \quad (41)$$

where μ_o is the membership function, f_0 is the *oth* objective function, and $f_0^{\min}$, $f_0^{\max}$ are its minimum and maximum values, respectively.

- Calculate the normalized membership value:

$$\mu^k = \frac{\sum_{o=1}^3 \mu_o^k}{\sum_{l=1}^{HMS} \sum_{o=1}^3 \mu_o^l}. \quad (42)$$

The solution having the maximum value of μ^k represents the best compromise solution.

b)   The proposed method to solve the multi-objective problem

The proposed method is a mixture of mathematical methods to find a solution that can be considered as the best among the solutions, because this method depends on two parts:

The first part of this method is to divide the solution domains into several domains and make it a two-dimensional matrix at a two-objective function and a three-dimensional one in case of a three-objective function so that for each domain contains a certain number of solutions that are found by Pareto fronts, Therefore, there is a high probability that an optimal solution is found in the domain containing the largest number of solutions. The following equations model the first part of the method:

$$P = \max \begin{pmatrix} A_1^1 & \cdots & A_1^i \\ \vdots & \ddots & \vdots \\ A_1^j & \cdots & A_j^i \end{pmatrix}, \quad (43)$$

$$P = \max \begin{bmatrix} & & A_1^{k^1} & \cdots & \cdots & A_1^{k^i} \\ & \cdot^{\cdot} & \vdots & & \cdot^{\cdot} & \vdots \\ A_1^{1^1} & \cdots & \cdots & A_1^{1^i} & & \vdots \\ \vdots & & \vdots & \vdots & & \vdots \\ \vdots & & A_j^{k^i} & \vdots & \cdots & A_j^{k^i} \\ \vdots & \cdot^{\cdot} & & \vdots & \cdot^{\cdot} & \\ A_j^{1^i} & \cdots & \cdots & A_j^{1^i} & & \end{bmatrix} \quad (44)$$

where

$$\begin{cases} A_j^i = ([f_i^{(i-1)}; f_i^{(i)}], [f_2^{(j-1)}; f_2^{(j)}]), \\ A_j^k = ([f_i^{(i-1)}; f_i^{(i)}], [f_2^{(j-1)}; f_2^{(j)}], [f_3^{(k-1)}; f_3^{(k)}]) \\ C \in A_j^i \, or \, A_j^{k^i} \end{cases}$$

$$(45)$$

and

$$\begin{cases} B_o = \dfrac{f_{\max_o} - f_{\min_o}}{N_d}, \\ \\ f_o^{((iorjork)-1)} = f_{\min_a} + ((iorjork) - 1) * B_o, \\ f_o^{(iorjork)} = f_{\min_a} + (iorjork) * B_o, \\ \qquad N_d = i = j = k, \end{cases}$$

$$(46)$$

Where (A_j^i) and $(A_j^{k^i})$ is the cell of solutions in 2 dimensions and 3 dimensions respectively, (B_o) is the distance between domains of the objective functions, (i, k, j) and (N_d) are the numbers of the domains and (o) is the objective functions respectively and (f_{max}, f_{min}) are the maximum and minimum values of the objective function existing in the harmonic memory with (C) the number of the solutions in each cell (A) and (P) is the cell that contains the most solutions.

After finding the domain with the most solutions, a second part of the method comes where we use the method of a point that is closer to other points, so that a chosen point does not prefer one goal to another, which is the same principle of non-dominance, and from there we consider the obtained point as an optimal solution. The expression of the second part of the proposed method is;

$$\begin{cases} G = \min \begin{pmatrix} d_1 \\ \vdots \\ d_x \end{pmatrix}, \\ \\ d_x = \sqrt{\sum_0 (f_0^x - f_0^1)^2} + \cdots \sqrt{\sum_0 (f_0^x - f_0^y)^2}, \end{cases}$$

$$(47)$$

Where (d_x) is the sum of the distances between the selected solution (x) and the other solutions (y) in cell P and (G) is the optimum solution.

c) The geometric median The geometric median (or geometric center) is a measure of location for a set of points in a multidimensional space. It represents the point that minimizes the sum of the squared Euclidean distances to each of the points in the set, as shown in Equation (47).

3.2. Solution process

The process of generating the optimal solution for optimizing the design of a three-phase squirrel cage induction motor from the HS is shown in Figure 4. According
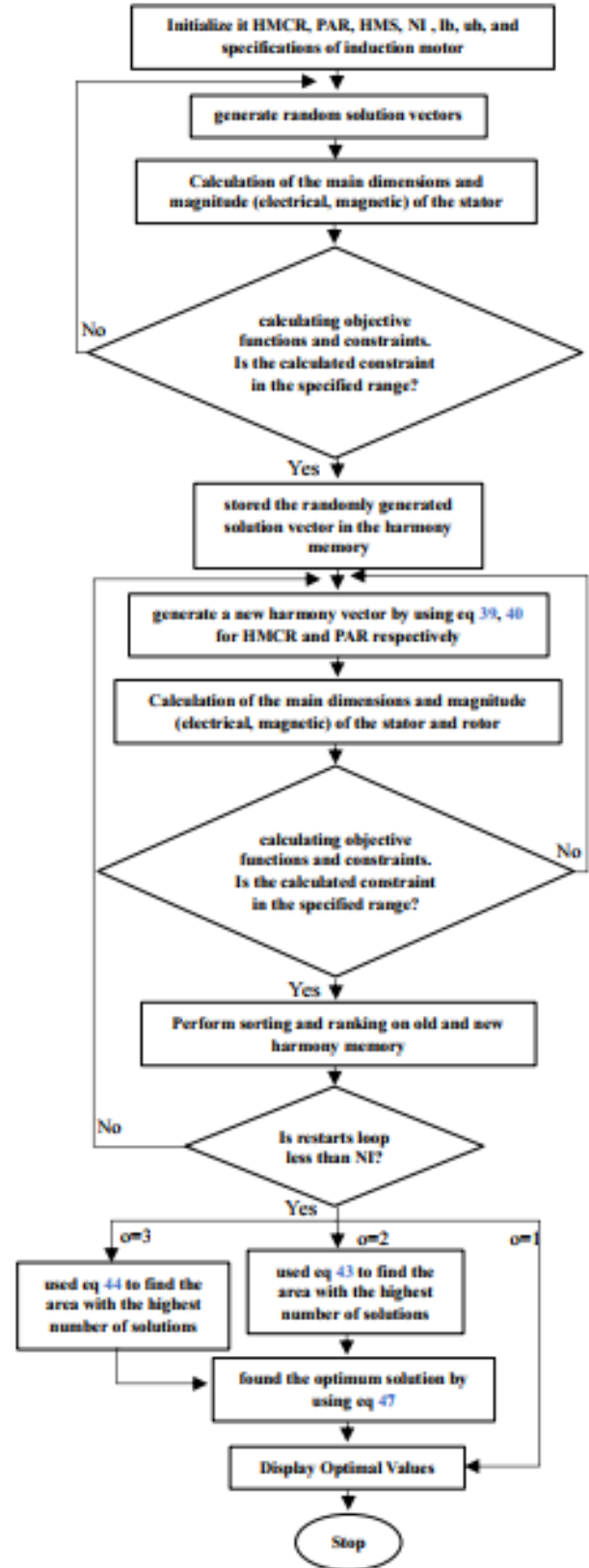

Fig. 4: Harmonic search algorithm used to optimize the design problem of a single-objective or multi-objective induction motor.

to Figure 4, the proposed approach to optimize the IM problem is described in the following steps:

1. Entering the parameters of HS they are lb, ub and choosing the size of the harmony memory HMS, the rate of consideration of the harmony memory $HMCR$ and the rate of pitch adjustment PAR, and the maximum number of improvisations NI. In addition, the entry of IM data.

2. Randomly generated solution vectors are used to calculate the main dimensions and quantities (electrical, magnetic) of the stator and rotor, in addition to calculating the selected constraints.

3. The examination if the constraints resulting from the generated solution vector are in the range given in section 2.4, if they are not in this range go back to the previous step.

4. Initialization of the HM harmony memory by storing the solution vectors that fulfill the condition of the previous step and which is named $HM1$.

5. Starting the improvisation.

6. Improving the new solution vector by $HMCR$ and PAR, as explained in section 3.1.3, the same steps of step 2 are done, the solution vector are used to calculate the main electrical and magnetic dimensions and magnitudes (of the stator and rotor), along with calculating the selected constraints.

7. In the same way as in step 3, the examination of whether the constraints resulting from step 6 are within the specified range. If so, this solution vector is stored by a new HM. Which is named by $HM2$, if not returned in the previous step.

8. The two $HM1$ and $HM2$ are merged to give a combined harmony memory between the two, $HM3 = HM1 \cup HM2$, then perform the sorting and non-dominated ranking on the combined harmony memory to choose the best harmony memory among the combined solution vectors, for the next improvisation. This step is well detailed and explained in [26].

9. The stopping conditions are checked if the number of improvisations has been reached at the maximum NI, go to the next step. Otherwise, return to step 6 with HM which is found by step 8 becomes new $HM1$.

10. To find the best solution vector drawn by the Pareto optimal set there are three possible cases: a) If the $o = 1$ or the mono-objective function, the best solution what is classified first in HM, and to pass it to the step 12. b) If the $o = 2$ or

bi-objective function, we used Eq (43) to extract the cell A_j^i that contains the most solutions, go to the next step. c) If the $o = 3$ or the tri-objective function, Eq (44) was used to extract the cell $A_j^{k^i}$ that contains the most solutions, go to the next step.

11. To extract the best solution in b, c Eq (47), was used which represents the closest point compared to the other points.

12. Display the optimal values.

4. Results and discussion

The HS algorithm is used to test the robustness of the proposed method for solving the multi-objective problem and obtaining the optimal results for IM. For this purpose, five case studies are defined to optimize the three objective functions, namely efficiency, total active mass of the motor and rated torque. The case studies are: 1st case, it's the use of HS algorithm to improve the three objectives individually, the other cases focused on the methods that is solving the multi-objective problem, namely the proposed method, fuzzy membership approach employed in [12,13] and the Geometric Median (GM) method,with the parameters using in the HS algorithm in the previous cases being **$HMS= 200,NI = 500,HMCR =0.5,PAR =0.2$**. In addition, it should be noted that all the results obtained by the algorithms are compared with the conventional design results already discussed in Section 2. All simulations were implemented in MATLAB and run on an Intel core-i5 1.80GHz personal computer.

Case 1: use the algorithm HS to optimize the three objectives individually
Table 4 and Table 5 show the simulation results obtained by the three objectives individually by the HS algorithm and the initial engine for this case. As can be seen in Figure 5 that the fitness value converged after 100 iterations to obtain the optimal design for each objective. In addition, the HS algorithm gives favorable results in a faster time as shown in Table 5.

Case 2: Maximizing efficiency and rated torque
In this case, two competing objectives, namely efficiency and rated torque, were considered. This multi-objective optimization problem was solved by the HS algorithm which is given the Pareto optimal solution, this solution is segmented by using the 1st part of the proposed method to obtain two dimensional cells as was presented in Figure 6(a). In addition, this figure shows the cell that has the largest number of solutions in the range of rated torque between 121.7 $N.m$ and 122.2 $N.m$ and efficiency between 0.9073 and 0.9115,

(a)

(b)

(c)
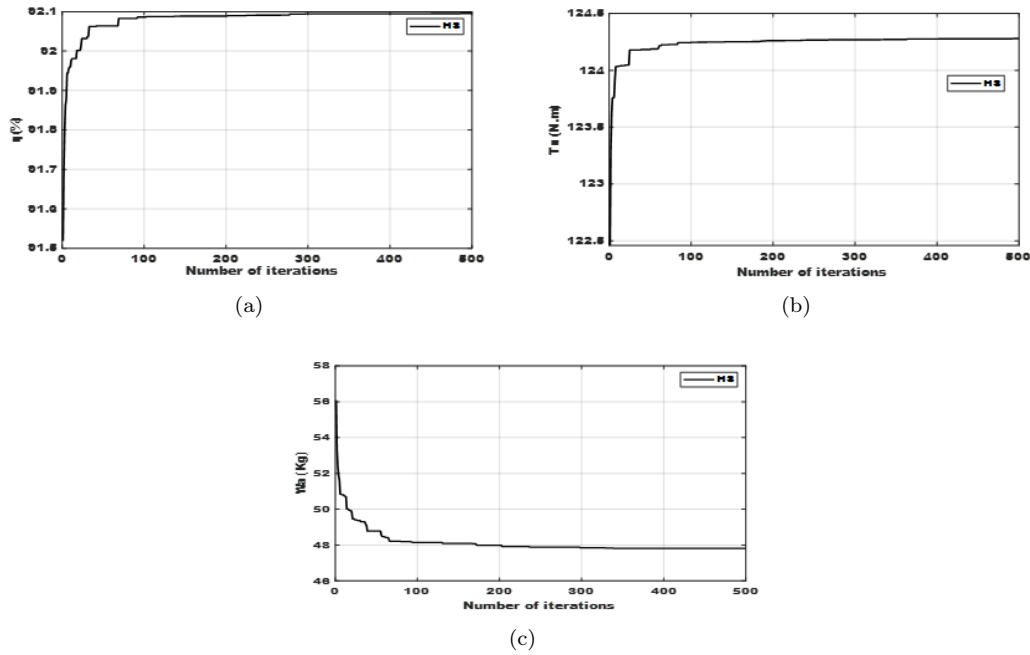
Fig. 5: Convergence of the objective function using harmony search algorithms (a) efficiency (b) rating torque (c) total active mass.

Tab. 4: Design parameters for the perimeter case.

Parameter	IM	Mono-objective		
		$W(HS)$	$Tu(HS)$	$\eta(HS)$
Z_{Qs}	36	36	36	32
$l(mm)$	165	161	164.3	171.5
$\delta(mm)$	0.243	0.211	0.47	0.251
$Em(V)$	387.42	370.49	386.05	370.5
$b_{1cs}(mm)$	4.23	4	4.4	5.5
$h(mm)$	24.72	16.01	16.01	21.06
$b_{1r}(mm)$	5.8	5.3	4.5	6.3
$h_{2r}(mm)$	16.78	10.02	10.03	13.69
$\hat{B}_{ys}(T)$	1.97	2	1.94	1.43
$\hat{B}_{yr}(T)$	1.8	1.9	1.45	1.63

which represents 30 solutions in total. Furthermore, it should be noted that the smallest value in both domains is better than the one found in the initial motor, so this shows that all the solutions of this cell represent optimal solutions as was shown in Figure 6(b). Figure 7 shows the Pareto front and the solutions by the proposed method (MP) in red, the method by the fuzzy membership approach in green and the Geometric Median (GM) method in black. This figure shows that the proposed method gives better solution compared to the other methods because it finds balanced solution between the two objectives. Table 6 gives the best solution vectors for maximum efficiency and maximum rated torque and Table 7 gives the optimal motor performance for this case.

Case 3: Maximizing efficiency and minimizing total active mass

In this case, the total active mass is considered in-stead of the rated torque. In the same way as in the previous case, these two competing objective functions were optimized simultaneously by the HS algorithm. Figure 8(a) shows the cell with the highest number of solutions in the range of total active mass between $-56.45Kg$ and $-54.49Kg$ and efficiency between 0.9092 and 0.9108, which represents 36 solutions in total. Furthermore, all solutions in this cell shown in Figure 8(b), and by this figure, it can be seen that the smallest value in both domains is higher than the one found in the initial motor. Figure 9 like Figure 7 represented the Pareto front and the solutions by proposed method (PM) in red, the method by fuzzy membership approach in green and the method of Geometric Median (GM) in black This figure shows that the proposed method gave the most balanced solution between the two objectives compared to the other methods. Table 6 gives the best solution vectors for maximum efficiency and minimum total active mass and Table 7 gives the optimal engine performance for this case.

Case 4: Maximizing the rated torque and minimizing the total active mass

In this case, two competing objectives, namely total active mass and rated torque, were considered. Similarly in case 3-4 this problem was optimized by the HS algorithm. Figure 10(a) shows the cell that has the highest number of solutions in the range of total active mass between $-48.24Kg$ and $-48.05Kg$ and rated torque between 124.27 $N.m$ and 124.28 $N.m$, which represents 34 solutions in total. Furthermore, all the solutions in this cell shown in Figure 10(b), and Figure

Tab. 5: Design parameters for the perimeter case.

| Parameter	Symbol	IM	Mono-objective		
			$W(HS)$	$Tu(HS)$	$\eta(HS)$
The outer diameter	$Dse(mm)$	266.55	242.9	249.1	284.1
The inner diameter	$Ds(mm)$	163.99	159.93	163.97	170.44
Flux density in the air gap	$B\sigma(T)$	0.84	0.87	0.89	0.79
Flux density in the stator tooth	$Bds(T)$	1.61	1.64	1.76	1.84
Flux density in the rotor tooth	$Bdr(T)$	1.93	1.87	1.64	1.9
Total active mass	$Wa(Kg)$	**63.9**	**47.8**	53.45	75.2
Stator current density	$Js(A/mm^2)$	3.65	6.648	6.173	3.001
Rotor current density	$Jr(A/mm^2)$	3.87	5.929	6.5	3.001
Power factor	$\cos(\phi)$	0.861	0.86	0.86	0.891
Rated current	$Is(A)$	19.84	20.41	20.48	18.85
Starting current	$Isd(A)$	106.92	113.07	109.39	123.62
Starting torque	$Td(N.m)$	98.77	162.54	168.91	99.2
Rating torque	$Tu(N.m)$	**121.07**	123.56	**124.28**	119.91
Efficiency	$\eta\%$	**90.57**	88.162	87.866	**92.096**
Time per iteration(s)			**1.15**	**1.58**	**0.83**

(a)

(b)
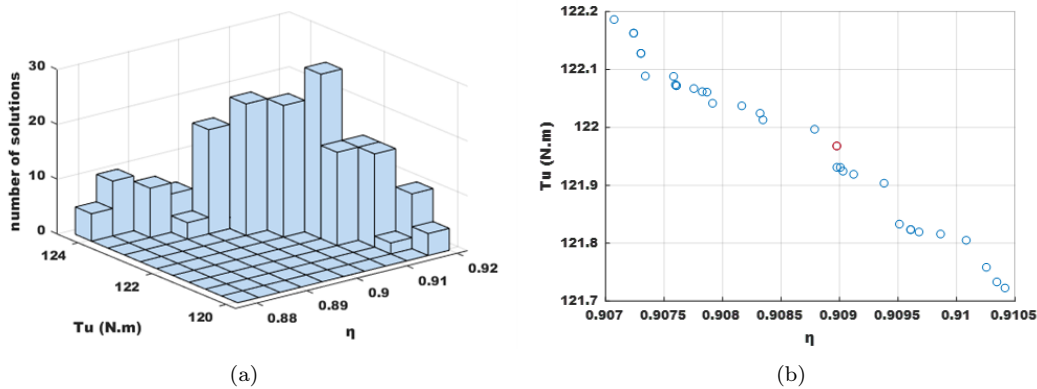
Fig. 6: Segmentation of the pareto front using the method proposed for case 2 (a) variation in pareto front solutions for rated torque and efficiency (b) Magnification of the cell that contains a larger number of solutions with the optimal solution in red.
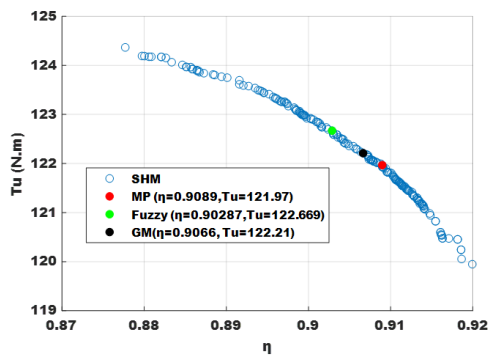
Fig. 7: Pareto optimal solutions for rated torque and efficiency.

11 represented the Pareto front of all the solutions that is obtained by the HS algorithm in blue with the solutions by proposed method (PM) in red, the method by fuzzy membership approach in green and the Geometric Median (GM) method in black. This figure shows that all these solutions are superior to the one found in the initial motor. In addition, this figure demonstrate that the proposed method gave the most balanced solu-

tion between the two objectives compared to the other methods. Table 6 gives the foremost solution vectors for maximum useful torque and minimum total active mass and Table 7 gives the optimal engine performance for this case.

Case 5: Maximizing efficiency and rated torque and minimizing total active mass
In this case, the three competing objectives were considered. These three objectives were optimized simultaneously by the HS algorithm that it gives the Pareto optimal solution. This solution makes segment by using the 1st part of the proposed method to obtain cells of three dimensions, each dimension is represented in Figure 12(a). In addition, this figure shows the cell that has the largest number of solutions in the range of rated torque between 121.5 $N.m$ and 121.8 $N.m$, efficiency between 0.906 and 0.909 and total active mass between $-60Kg$ and $-58Kg$, which represents 9 solutions in total. Furthermore, it is worth noting that the smallest value in the three domains is better than the one found in the initial motor, so this shows that all the solutions of this cell represent optimal solutions as was

Tab. 6: Design parameters for the perimeter case.

Parameter	IM	HS-two-objectif									HS-three-objectif		
		(Wa, Tu)			(Wa, η)			(Tu, η)					
		M^1	M^2	M^3	M^1	M^2	M^3	M^1	M^2	M^3	M^1	M^2	M^3
Z_{Qs}	36	36	36	36	36	36	36	36	36	36	36	36	36
$l(mm)$	165	161.8	161.1	162.2	162.5	161.9	161.9	165.6	164.6	161.5	163.2	162.7	162.9
$\delta(mm)$	0.243	0.214	0.216	0.213	0.204	0.202	0.209	0.32	0.356	0.295	0.244	0.295	0.379
$Em(V)$	387.42	370.55	370.8	371.23	370.54	370.54	370.57	371.07	370.53	372.89	378.67	370.53	376.35
$b_{1cs}(mm)$	4.23	4	4.1	4.3	5.3	5.2	5.2	5.6	5.3	5	5.2	5.3	5.2
$h(mm)$	24.72	16.049	16.026	16.04	18.68	18.43	19.38	22.48	23.32	20.86	20.05	19.54	16.01
$b_{1r}(mm)$	5.8	4.8	4.5	4.6	6	6	6	5	4.8	4.5	6	5.6	5
$h_{2r}(mm)$	16.78	10.016	10.594	10.03	14.89	15.51	15.33	10.03	10.1	10.03	10.08	10.1	10.1
$Bys(T)$	1.97	1.99	1.99	1.99	1.83	1.86	1.83	1.5	1.57	1.53	1.75	1.66	1.73
$Byr(T)$	1.8	1.89	1.88	1.9	1.89	1.88	1.9	1.46	1.7	1.89	1.63	1.83	1.74

$^{*}M^1$: the proposed method, M^2: the Geometric Median, M^3: fuzzy membership approach
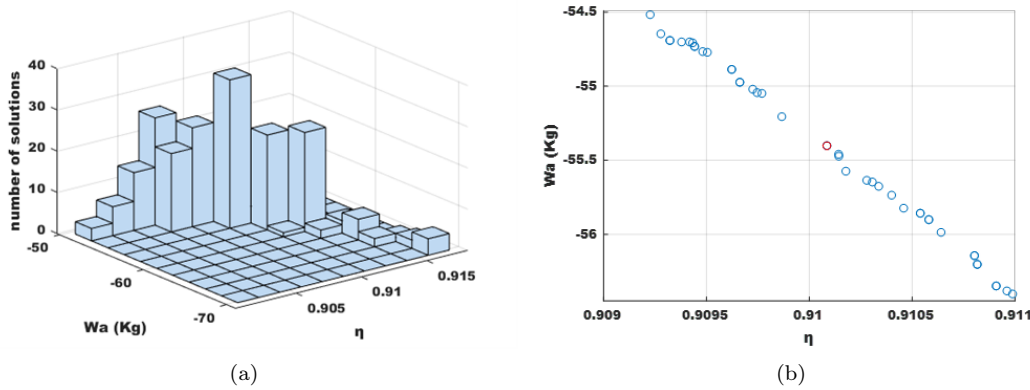

(a)

(b)

Fig. 8: Segmentation of the pareto front using the method proposed for case 3 (a) variation in pareto front solutions for total active mass and efficiency (b) Magnification of the cell that contains a larger number of solutions with the optimal solution in red.
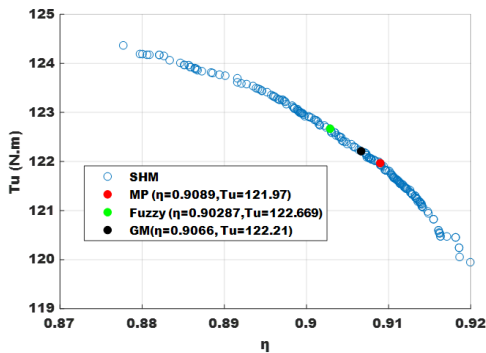

Fig. 9: Pareto optimal solutions for total active mass and efficiency.

shown in Figure 12(b). Figure 13 represents the Pareto front and the solutions by the proposed method (PM) in red, the method by fuzzy membership approach in green and the method of Geometric Median (GM) in black. This figure shows that the proposed method gives better solution compared to the other methods because it finds a balanced solution between the three objectives. Table 6 gives the best solution vectors for maximum efficiency and maximum useful torque and

Table 7 gives the optimal motor performance for this case.

Table 8 shows the effectiveness of the methods used and the rate of improvement compared to the initial case. It is worth noting that the proposed method is the most efficient in all cases for choosing an optimal solution between the GM and Fuzzy methods. Indeed, Table 8 shows that the Fuzzy method does not give good results when there is strong competition between objectives, where the increase is low, such as efficiency and rated torque, because it is attracted to the objective with the highest value, which gives an inappropriate optimal solution for this method. As for the GM method, it chooses an average value on the Pareto front, which is not an optimal solution. Therefore, it can be seen that when the increase is small, as in cases 2 and 5, it chooses the point that increases the efficiency by less than 0.1%, which means that there is no improvement in efficiency. Unlike the proposed method, which relies on the density of solutions, it gives an optimal solution that balances the objectives. Therefore, it can be concluded that the proposed method is the best for choosing points on the Pareto front compared to the Fuzzy method used in [12, 13] and GM. With an

Tab. 7: Design performance for cases 2-5.

Parameter	IM	HS-two-objectif									HS-three-objectif		
		(Wa, Tu)			(Wa, η)			(Tu, η)					
		M^1	M^2	M^3	M^1	M^2	M^3	M^1	M^2	M^3	M^1	M^2	M^3
The outer diameter $Dse(mm)$	266.55	243.5	243.2	244.1	253.9	252.3	254.9	274.3	272.7	266.8	260.5	260.8	252.4
The inner diameter $Ds(mm)$	163.99	160.74	160.05	161.13	161.4	160.8	160.82	164.82	163.9	160.6	162.21	161.8	162.3
Flux density in the air gap $B\sigma(T)$	0.84	0.88	0.88	0.87	0.78	0.78	0.78	0.77	0.79	0.82	0.8	0.79	0.82
Flux density in the stator tooth $Bds(T)$	1.61	1.65	1.7	17	1.83	1.83	1.83	1.87	1.85	1.85	1.84	1.86	1.89
Flux density in the rotor tooth $Bdr(T)$	1.93	1.73	1.64	1.63	1.9	1.9	1.9	1.53	1.52	1.54	1.91	1.79	1.66
Total active mass $Wa(Kg)$	**63.9**	**48.16**	**48.21**	**48.68**	**55.41**	**54.73**	**56.14**	68.5	66.37	61.16	**59.36**	**58.62**	**53.06**
Stator current density $Js(A/mm^2)$	3.65	6.638	6.424	6.257	4.175	4.301	4.05	3.14	3.15	3.79	3.794	3.928	5.07
Rotor current density $Jr(A/mm^2)$	3.87	6.499	6.499	6.484	3.51	3.495	3.5	4.9	5.21	5.71	4.462	4.672	5.21
Power factor $\cos(\phi)$	0.861	0.862	0.866	0.861	0.877	0.873	0.873	0.896	0.89	0.891	0.9	0.9	0.88
Rated current $Is(A)$	19.84	20.44	20.31	20.41	19.39	19.48	19.47	19	19.17	19.24	18.96	19.21	19.55
Starting current $Isd(A)$	106.92	110.83	108.14	111.63	112.57	113.41	113.1	103.2	103.5	104.5	105.6	108.57	109.9
Starting torque $Td(N.m)$	98.77	171	168.39	173.92	99.37	99.7	99.55	119.96	126.9	138.4	112.95	123.94	139.8
Rating torque $Tu(N.m)$	**121.07**	**124.28**	**124.28**	**124.36**	120.72	120.7	120.6	**121.97**	**122.21**	**122.66**	121.6	121.6	122.6
Efficiency $\eta\%$	**90.57**	87.82	88.02	88.043	**91.01**	**90.94**	**91.08**	**90.898**	**90.66**	**90.28**	90.73	90.66	89.68
Time per iteration(s)			1.54			1.31			1.32			1.16	

$^\dagger M^1$: the proposed method, M^2: the Geometric Median, M^3: fuzzy membership approach.

improvement compared to the initial case in the case of three-objective optimization of 0.4377% for rated torque, 0.1766% for efficiency and 7.1048% for active mass.

5. Conclusion

This paper presents the multi-objective optimization which uses the harmony search algorithm to deal with the design of induction motors. Firstly, the three ob-

Tab. 8: The optimization rate for each method compared to the initial case in cases 2-5.

Method	Case 2		Case 3		Case 4		Case 5		
	$\eta\%$	$Tu\%$	$\eta\%$	$Wa\%$	$Wa\%$	$Tu\%$	$\eta\%$	$Tu\%$	$Wa\%$
The proposed method	0.3621	0.7433	0.4858	13.286	24.632	2.6513	0.1766	0.4377	7.1048
The GeometricMedian	0.0993	0.9416	0.4085	14.35	24.553	2.6513	0.0993	0.4377	8.2629
Fuzzy membership approach	-0.3201	1.3132	0.5631	12.143	23.818	2.7174	-0.9826	1.2637	16.964

(a)   (b)
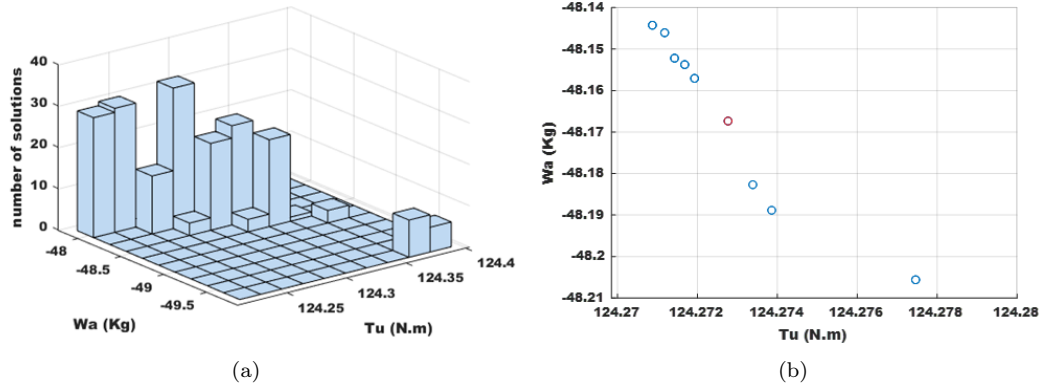
Fig. 10: Segmentation of the pareto front using the method proposed for case 4 (a) variation in pareto front solutions for total active mass and rated torque (b) Magnification of the cell that contains a larger number of solutions with the optimal solution in red.
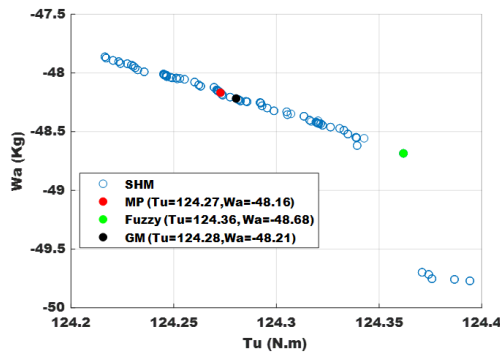

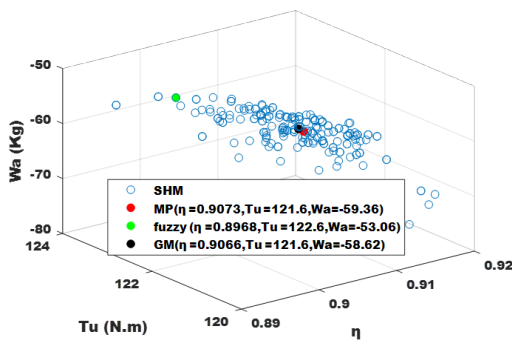**Fig. 11:** Pareto optimal solutions for total active mass and rated torque.

jective functions that are composed of efficiency, rated torque and total active mass were taken separately as objective function in single objective optimization by HS algorithm. The results obtained show that the HS algorithm used gives good results in a shorter time with fewer iterations. Then, the objective functions were solved as a multi-objective problem by the MOHS algorithm. To identify the best compromise solution by Pareto optimal solutions fuzzy membership approach method, Geometric Median (GM) method and proposed method were used. According to the simulation results, the proposed method is able to give the best and most balanced solution between the objective functions in the Pareto optimal solutions compared to the other methods for the IM problem with different objectives.

References

[1] PRAKASH, R., M. J. AKHTAR, R. K. BEHERA, S. K. PARIDA. Design of a three-phase squirrel cage induction motor for electric propulsion system. *IFAC Proceedings Volumes*. 2014, vol. 47, iss. 1, pp. 801-806. DOI: 10.3182/20140313-3-IN-3024.00242.

[2] AISHWARYA, M. et R. M. BRISILLA. Design of Energy Efficient Induction motor using ANSYS software. *Results in Engineering*. 2022, vol. 16, p. 100616. DOI: 10.1016/j.rineng.2022.100616.

[3] ALBERTI, L., N. BIANCHI, A. BOGLIETTI, A. CAVAGNINO. Core axial lengthening as effective solution to improve the induction motor efficiency classes. *IEEE Trans. Ind. Appl.* 2015, vol. 50, iss. 1, pp. 218–225. DOI: 10.1109/TIA.2013.2266632.

[4] PRAKASH, P. S., P. ARAVINDHABABU. Multi-objective Design of Induction Motor using Harmony Search Optimization. *International Journal of Computer Applications*. 2015, vol. 116, iss. 23. DOI: 10.5120/20503-2222.

[5] GEEM, Z. W., J. H. KIM, G. V. LOGANATHAN. A new heuristic optimization algorithm: harmony search. *Simulation*. 2001, vol. 76, iss. 2, pp. 60-68. DOI: 10.1177/003754970107600201.

[6] INGRAM, G. and T. ZHANG. Overview of Applications and Developments in the Harmony Search

(a)

(b)
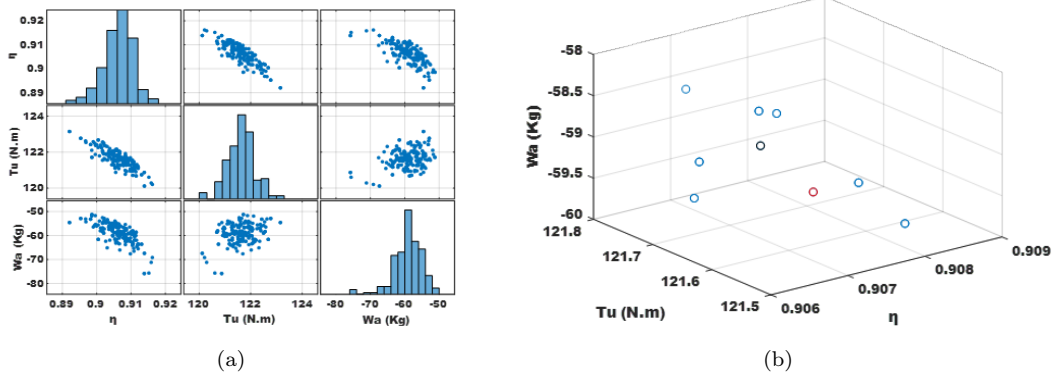
Fig. 12: Segmentation of the pareto front using the method proposed for case 5 (a) map of figures for the variation among the three objective functions total active mass, rated torque and efficiency (b) Magnification of the cell that contains a larger number of solutions with the optimal solution in red.

Fig. 13: Pareto optimal solutions for total active mass and rated torque.

Algorithm, *Music-Inspired Harmony Search Algorithm: Theory and Applications*. 2009, pp. 15–37. DOI: 10.1007/978-3-642-00185-7_10.

[7] YANG, X.-S. Harmony search as a metaheuristic algorithm. *Music-inspired harmony search algorithm: theory and applications*. 2009, pp. 1-14. DOI: 10.1007/978-3-642-00185-7.

[8] GEEM, Z. W., K. S. LEE, Y. PARK. Application of Harmony Search to Vehicle Routing. *Am. J. Appl. Sci.* 2005, vol. 2, pp. 1552–1557. DOI: 10.3844/ajassp.2005.1552.1557.

[9] GEEM, Z. W. Multi objective Optimization of Time-Cost Trade-Off Using Harmony Search. *J. Constr. Eng. Manag. Asce.* 2010, vol. 136, pp. 711–716. DOI: 10.1061/(ASCE)CO.1943-7862.0000167.

[10] XU, H., X. Z. GAO, T. WANG, K. XUE. Harmony search optimization algorithm: application to a reconfigurable mobile robot prototype. *Recent advances in harmony search algorithm*. 2010, p. 11-22. DOI: 10.1007/978-3-642-04317-8_2.

[11] COELLO COELLO COELLO, Carlos A. A short tutorial on evolutionary multiobjective optimization. In: *International Conference on evolutionary multi-criterion optimization*. Berlin, Heidelberg: Springer Berlin Heidelberg, 2001. p. 21-40. DOI: 10.1007/3-540-44719-9_2.

[12] MELLAL M.A., A. SALHI, Multi-objective system design optimization via PPA and a fuzzy method, *Int. J. Fuzzy Syst.* 2021, vol. 23, pp. 1213–1221. DOI: 10.1007/s40815-021-01068-z

[13] MELLAL, M. A., E. ZIO, M. PECHT. Multi-objective reliability and cost optimization of fuel cell vehicle system with fuzzy feasibility. I*nformation Sciences*. 2023, vol. 640, p. 119112. DOI: 10.1016/j.ins.2023.119112

[14] BOLDEA, I., and S.A. NASAR. *The Induction Machine Handbook*. 2002. DOI: 10.1201/9781420042658

[15] JOKINEN, T., V. HRABOVCOVA and J. PYRHONEN. *Design of rotating electrical machines*. John Wiley & Sons, 2013. DOI: 10.1002/9781118701591.

[16] KHALGHANI, S., L. AARNIOVUORI and J. PYRHÖNEN. Evaluation of 5 kW Converter-Fed Induction Motor Losses by Analytical Calculation. In: 2*022 29th International Workshop on Electric Drives: Advances in Power Electronics for Electric Drives (IWED)*. Moscow, Russian Federation: IEEE, 2022. p. 1-6. DOI: 10.1109/IWED54598.2022.9722576.

[17] GMYREK, Z., A. BOGLIETTI and A. CAVAGNINO. Estimation of iron losses in induction motors: Calculation method, results, and analysis. *IEEE Transactions on Industrial Electronics*. 2009, vol. 57, iss. 1, pp. 161-171. DOI: 10.1109/TIE.2009.2024095.

[18] GAO, X. Z., T. JOKINEN, X. WANG, J. S. OVASKA and A. ARKKIO. A new harmony search method in optimal wind generator design. In: *The XIX International Conference on Electrical Machines-ICEM*. Rome, Italy: IEEE, 2010, pp. 1-6. DOI: 10.1109/ICELMACH.2010.5608219.

[19] LINDH P. , L. AARNIOVUORI, H. KARKKAINEN, M. NIEMELA and J. PYRHONEN. IM Loss Evaluation Using FEA and Measurements. In: *2018 XIII International Conference on Electrical Machines (ICEM)*. Alexandroupoli, Greece: IEEE, 2018, pp. 1220-1226. DOI: 10.1109/ICELMACH.2018.8507154.

[20] ÇUNKAŞ, M. Intelligent design of induction motors by multi objective fuzzy genetic algorithm. *Journal of Intelligent Manufacturing*. 2010, vol. 21, p. 393-402. DOI: 10.1007/s10845-008-0187-0.

[21] RICART, J., G. HÜTTEMANN, J. LIMA and B. BARAN. Multi objective Harmony Search Algorithm Proposals. Electron. *Notes Theor. Comput. Sci.* 2011, vol. 281, pp. 51–67. DOI: 10.1016/j.entcs.2011.11.025.

[22] TUO, S., L. YONG and F. DENG. A Novel Harmony Search Algorithm Based on Teaching-Learning Strategies for 0–1 Knapsack Problems. *Sci. World J.* 2014, vol. 2014, pp. 637412. DOI: h10.1155/2014/637412.

[23] FONSECA, C. M. and P. J. FLEMING. An Overview of Evolutionary Algorithms in Multi objective Optimization. *Evol. Comput.* 1995, vol. 3, pp. 1–16. DOI: 10.1162/evco.1995.3.1.1.

[24] DEB, K., A. PRATAP, S. AGARWAL and T. MEYARIVAN. A fast and elitist multiobjective genetic algorithm: NSGA-II. *IEEE Transactions on Evolutionary Computation*. 2022, vol. 6, iss. 2, pp. 182-197. DOI: 10.1109/4235.996017.

[25] DE LA FUENTE, D., M. A. VEGA-RODRIGUEZ and C. J. PEREZ. Automatic selection of a single solution from the Pareto front to identify key players in social networks. Knowl. *Based Syst.* 2018, vol. 160, pp. 228-236. DOI: 10.1016/j.knosys.2018.07.018.

[26] MOLINA-PÉREZ, D., et al. A novel multi-objective harmony search algorithm with pitch adjustment by genotype. *Applied Sciences*. 2021, vol. 11, iss. 19, pp. 8931 DOI: 10.3390/app11198931.